2001 CEDAR-SCOSTEP

Longmont, Colorado
June 17-22, 2001

Keynote Lecture

by Eugene Parker
University of Chicago, USA

What we need to know about Solar Variability

WHAT WE NEED TO KNOW ABOUT SOLAR VARIABILITY

E. N. Parker, Enrico Fermi Institute and Depts. of Physics and of Astronomy, University of Chicago

I Introduction

Solar Activity is only partially explored, its physics is only partially understood.

The Sun is a remote physics laboratory for large-scale MHD.

Space Missions

Subsurface conditions from GONG, SOHO.

Ground based Observatories

Small-scale solar activity exhibits short time scales, requiring large apertures for study.

The future Advanced Solar Telescope (AST)

Unfortunately, long term variability requires long term studies.

Proxy data, for which records already exist here at Earth.

Proxy Record

Isotope ratios, e.g. $^{18}O/^{16}O$ from ice cores, as a record of climate.

Radiogenic nuclei ^{14}C, ^{10}Be from old wood, ice cores. etc., as a record of cosmic ray intensity.

Cosmic rays play a major role in creating atmospheric ions, controlling atmospheric electricity.

Geomagnetic activity, aa index, is a measure of magnetic field in the solar wind, and hence at the Sun, and gives some idea of the suppression of cosmic rays.

We need to understand the role of solar activity in terrestrial climate if we are to:

1. Use climate as a proxy for solar activity.

2. Understand the role of solar activity in global warming.

A comprehensive global climate model is essential.

The most serious obstacles are limited computing power and the absence of cloud physics.
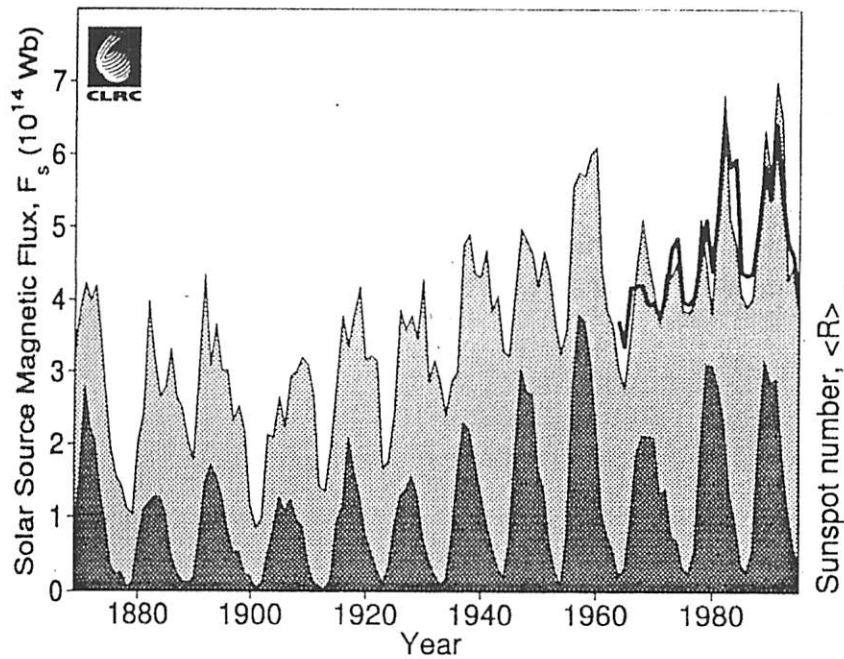
Figure 1: Variation of annual means of the coronal source flux F_s as derived from the aa index by the method of Lockwood et al. [1999a] (thin line bounding grey shaded area) and from interplanetary measurements of the radial component of the interplanetary magnetic field near Earth (thick line). The dark area gives the variation of the smoothed sunspot number.

CERN cosmic ray cloud physics experiment.

At the present time it appears that:

1. Solar activity was the principal warming influence 1900-1950

2. Accumulating greenhouse gases are the principal warming agent after 1970.

A comprehensive global climate model is essential for pressing ahead with the difficult (impossible?) political and economic tasks posed by global warming.

II Solar Structure

Sun is an opaque shroud wrapped around a thermonuclear core.

$$T \sim 1.5 \times 10^7 K, \rho \sim 115 \ gm/cm^3, \lambda \sim 2 \ Angstroms$$

Core is 2×10^{11} times brighter than the photosphere.

Assume same elemental abundances throughout, modified by thermonuclear creation and settling of He.

Hydrostatic equilibrium, Newtonian gravitation, radiative transfer, calculated opacities.

The theoretical model provides the speed of sound within 0.2 percent of the helioseismological model.

The models show convection in the outer 2×10^5 km (solar radius = 7×10^5 km). And that is where our story of solar activity begins.

The nonuniform rotation is driven by the convection.

The Coriolis force causes the convection to be cyclonic.

Magnetic fields are carried bodily by the convection and the nonuniform rotation.

The net result is a periodic $\alpha\omega$-dynamo.

Most of what we call solar activity is a consequence of the magnetic free energy.

Magnetic free energy can be rapidly converted into heat and

suprathermal flaring because equilibrium of

the magnetic stresses creates surfaces of tangential discontinuity

(current sheets). That is the basis for rapid reconnection.

III Solar Variability

Schwabe's 1844 discovery of the 11-year sunspot cycle.

Maunder's 1895 discovery of the long deep minimum 1645-1715.

Gleisberg's 1944, 1966 discovery of the 90 year cycle.

Eddy's 1973, 1976 substantiation of the Maunder Minimum.

Maunder Minimum in ^{14}C records.

10 such minima in the last 7000 years.

9 hyperactive periods.

The tendency of the mean annual temperature in the northern temperate zone to track solar activity.

Howard and LaBonte (1980) discover torsional oscillations

Helioseismology shows similar torsional oscillations in upper third of CZ (Komm, Howe, and Hill, 2000).

Angular velocity at base of CZ shows small oscillation with 1.3 year period.

Mouradian, et al (2000) find 10.7 cm radio signal with synodic period of 26.2 days at solar max. and 27.0 days at solar min.
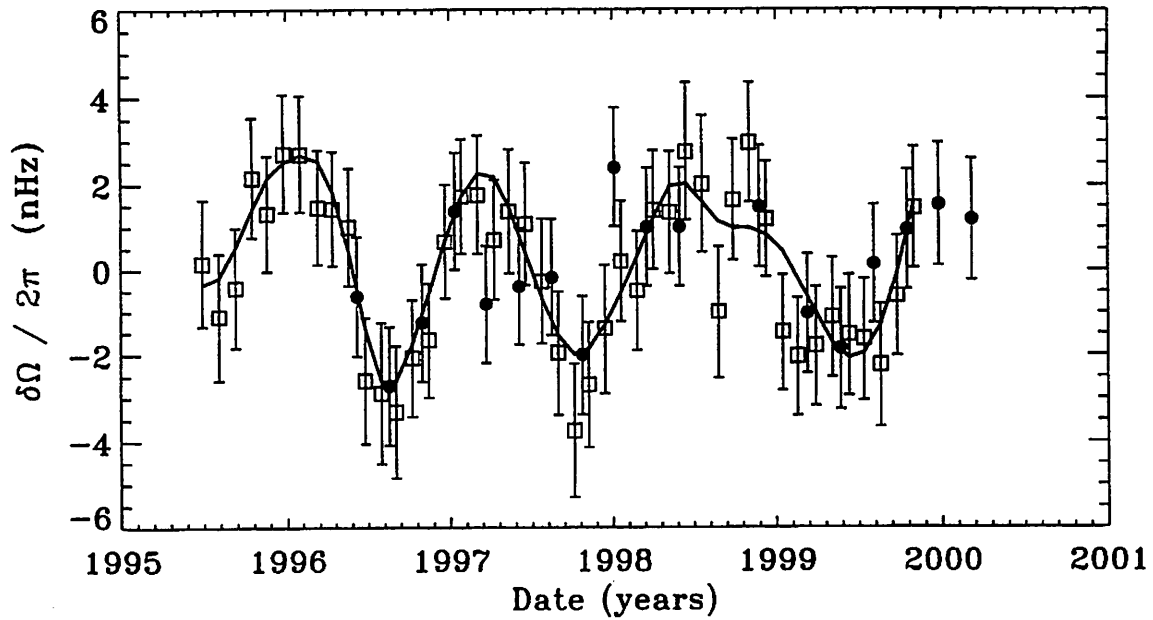
Figure 3. Variation with time of the residuals in equatorial rotation rate at radius $0.72R_\odot$. The symbols denote the data-inversion pairings: GONG-RLS (open squares), MDI-RLS (filled circles). The solid line represents the main component of an empirical mode decomposition of the GONG data.

In the vicinity of 2000, the Sun is more active than around 1900,

which was more active than the Dalton Minimum around 1800,

which was more active than the Maunder Minimum around 1700.

Lockwood, Stamper and Wild use the aa index to suggest that:

The magnetic flux through the solar surface increased by a factor of 1.6 from 1700 to 1900

and by a factor of 4 from 1700 to 2000.

Fligge, et al, (2000) and Lockwood and Stamper (1999) show that solar brightening tracks magnetic flux determined from aa index..

However de Toma and White (2000) note that cycle 23 seems to be anomalous in that respect.

Jimenez-Reyes, et al (2000) suggest frequency shift of p-modes as a useful solar index.

Damen and Sonett find 200 year period in ^{14}C production.

Dergachev, et al,(2000) find periods of 210 years, 420 years, 720 years, and 2400 years.

The 2400 year variation has been associated with the Little Ice age 15th-17th century and the cold period around 800 BC (Beer, et al, 1988).

Ice cores show a number of ancient glitches in ^{10}Be.

$^{18}O/^{16}O$ show abrupt onset of cold, followed by drop in CO_2.

IV Variations in Solar Brightness

Absolute radiometers (Willson and Hudson, 1991) show brightness variation with solar activity, $\Delta S/S \sim 1\text{-}2 \times 10^{-3}$.

What is the wavelength variation of ΔS?

What was $\Delta S/S$ during the Maunder Minimum?

What is the origin of ΔS at the present time?
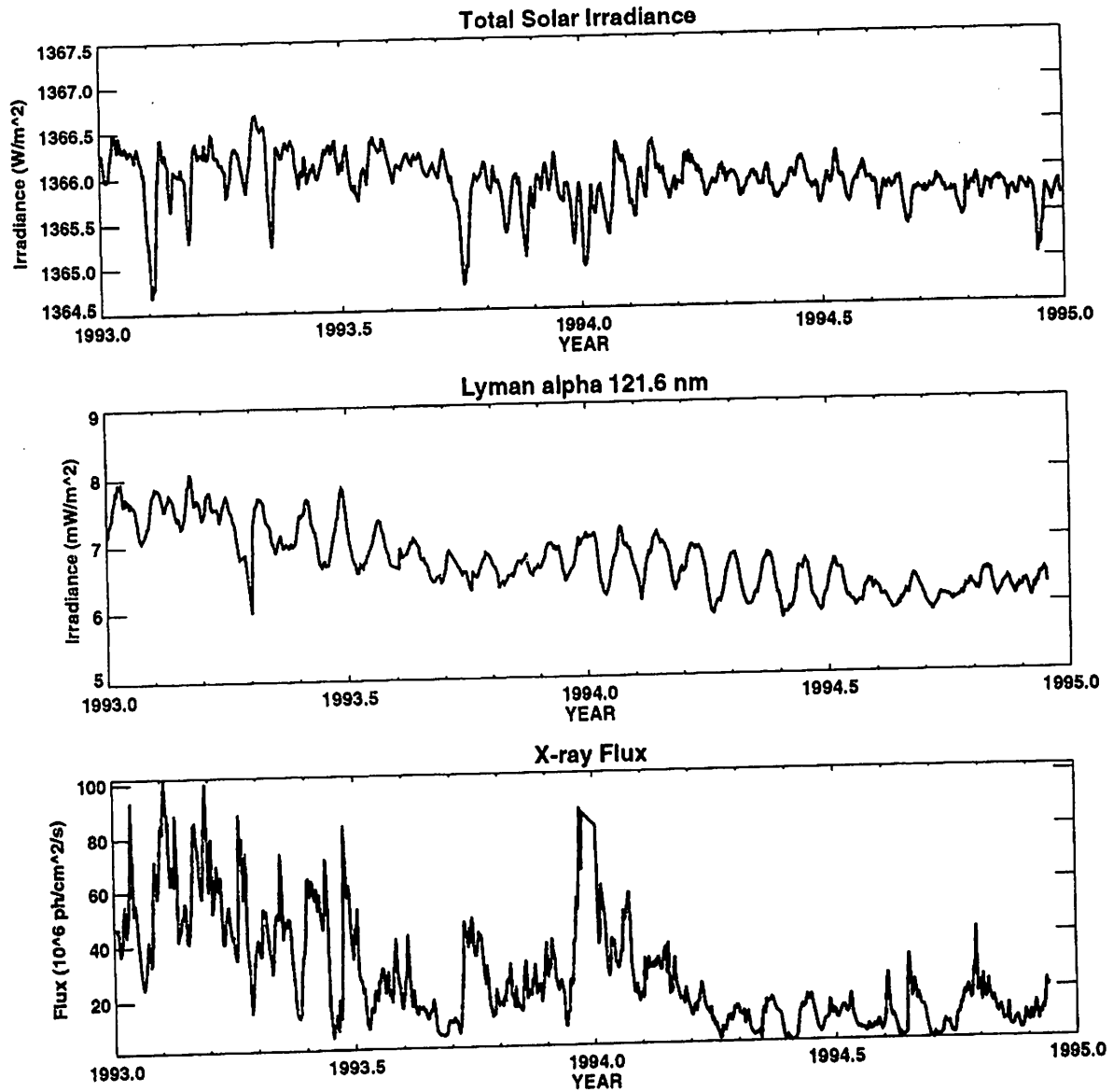
Figure 3. Comparison of TSI Variability with UV and X-ray Variability 1993-1995: TSI – all wavelengths (upper), Ly α - UV 121.6 nm (middle), 1-2 nm - X-ray (lower).
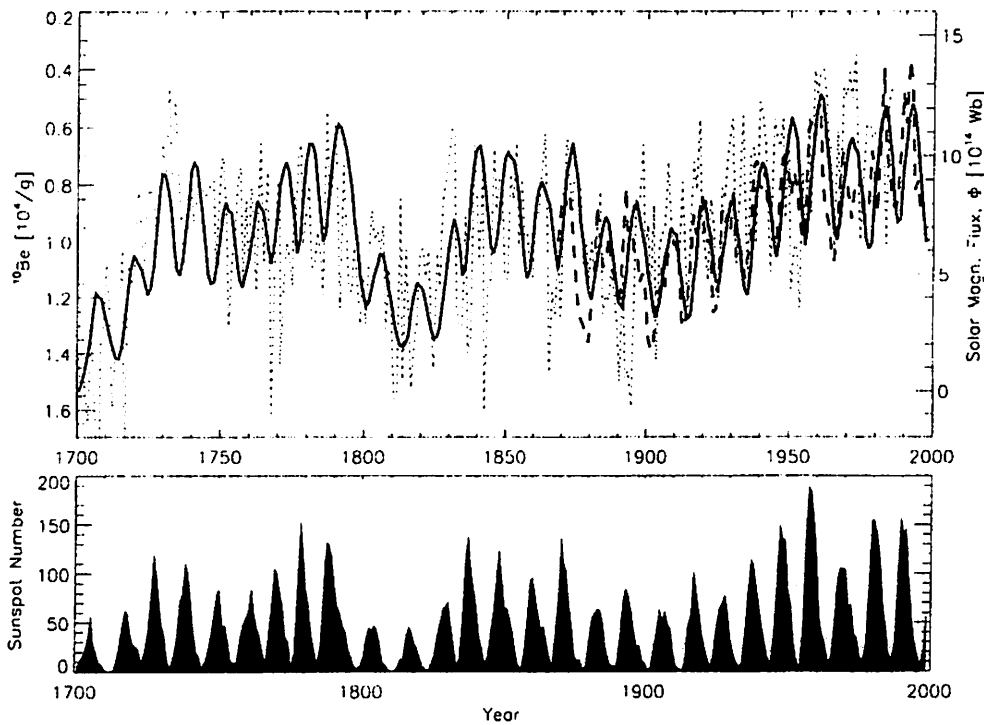
Figure 4. Evolution of the open magnetic flux at the solar surface since the end of the Maunder Minimum in 1700 as predicted by a model of the surface evolution of the Sun's magnetic field (upper panel, solid curve). For comparison, the flux of the interplanetary magnetic field (Lockwood et al., 1999) reconstructed from the geomagnetic aa-index (dashed curve) and the [10]Be concentration in ice cores (Beer et al., 1990) (dotted curve and left-hand, inverted scale) are also plotted. The interplanetary flux values have been multiplied by a factor of 2 in order to obtain the total unsigned flux. The [10]Be record has been plotted without any smoothing or filtering. For comparison, the lower panel shows the corresponding time sequence of the sunspot number, R (see Solanki et al., 2000 for details).

Spruit showed how individual magnetic fibrils appear as bright spots. Faculae are collections of magnetic fibrils.

Foukal and Lean showed that ΔS is 80-90 percent from sunspots, faculae, and network brightening.

So ΔS should be proportional to total magnetic flux and the aa index.

De Toma and White(2000) point out the cycle 23 seems to be an exception.

Sofia, et al (2000) argue that 11 year variation of ΔS arises from overall $\Delta T = 1.5K$ and $\Delta R = 15$ km.

Grey and Livingston infer from observations that $\Delta T = 1.5$ K.

We seem to have two "adequate" explanations for ΔS.
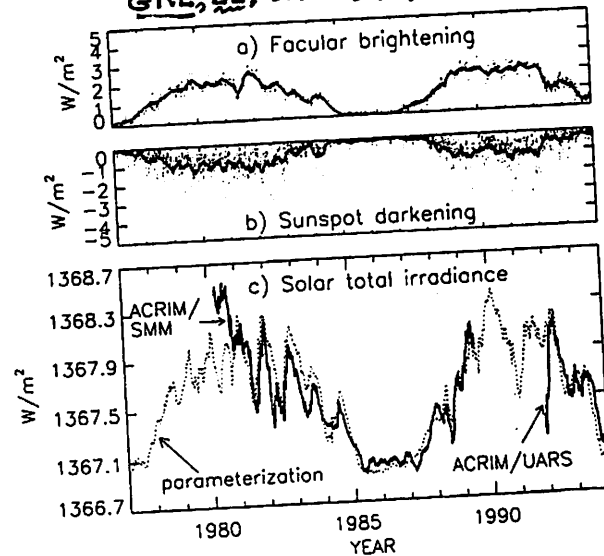
Figure 1. Shown are (a) bolometric facular brightening parameterized using He 1083 nm EW data, (b) sunspot darkening calculated from white light solar images, and (c) their net modulation of total irradiance during the Schwabe cycle, compared with measurements made by ACRIM on the SMM and UARS spacecraft, cross-calibrated using overlapping ERBS observations. Deviations of the SMM and UARS data from the reconstructed irradiances in 1980 and 1992, respectively, may reflect instrumental effects in the ACRIM data, since space-based radiometers are most susceptible to sensitivity changes during their first year of operation.
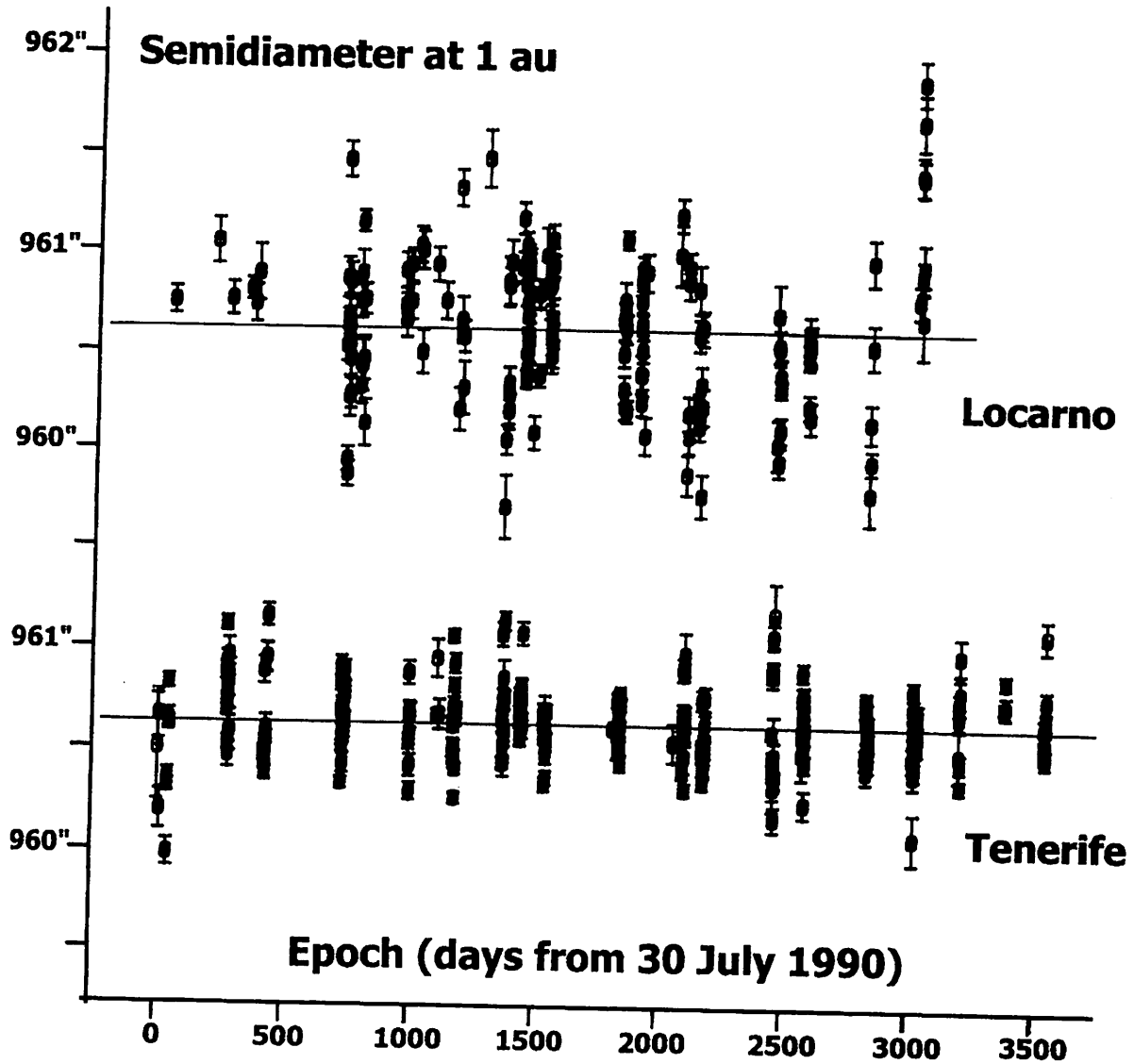
Figure 2: Semidiameter results from Locarno (1990-1998, top) and Tenerife (1990-2000, bottom). The daily mean values of the solar semidiameter (148 for Locarno, 232 for Izaña) are plotted as a function of time. One-sigma error levels are indicated by error bars (which, however, due to the relatively small dispersion of the diagram, mostly blend with their neighbors). Time is reckoned in days from 30 July 1990 0 UT, so that, e.g., 04 April 2000 0:00 UT is 3536.0 days from the initial epoch. The horizontal clustering of points reflects the distribution of the observing campaigns over the years (no drift observations were made during the winter season, when the conditions use to be fairly bad at both sites).

Evolution in time of the diameter of the Sun
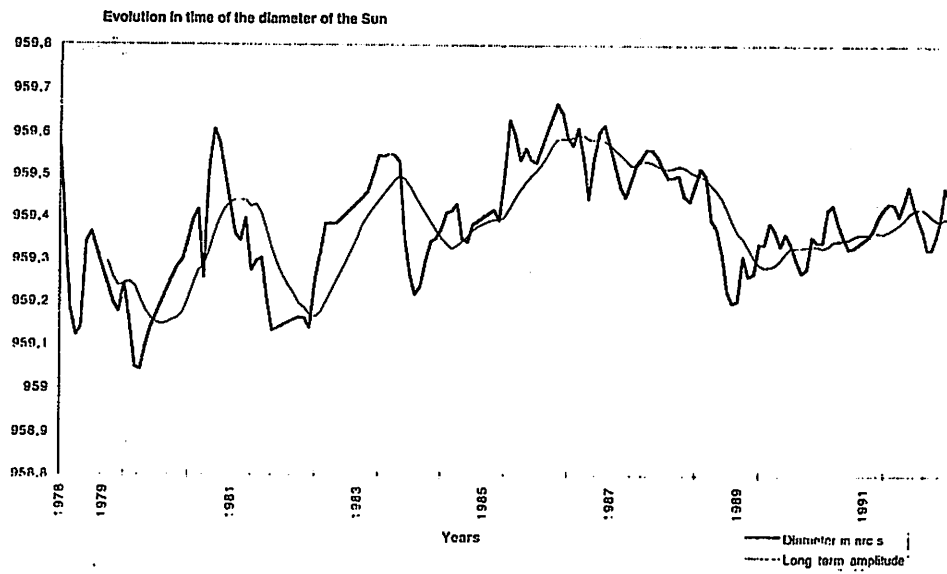
Figure 1. The solar diameter variations as shown from the measurements of F. Laclare at the Calern Observatory. The long-term amplitude is also plotted. An oscillation of mean amplitude 0.5 arc sec appears, which is out-of-phase with the solar activity cycle.
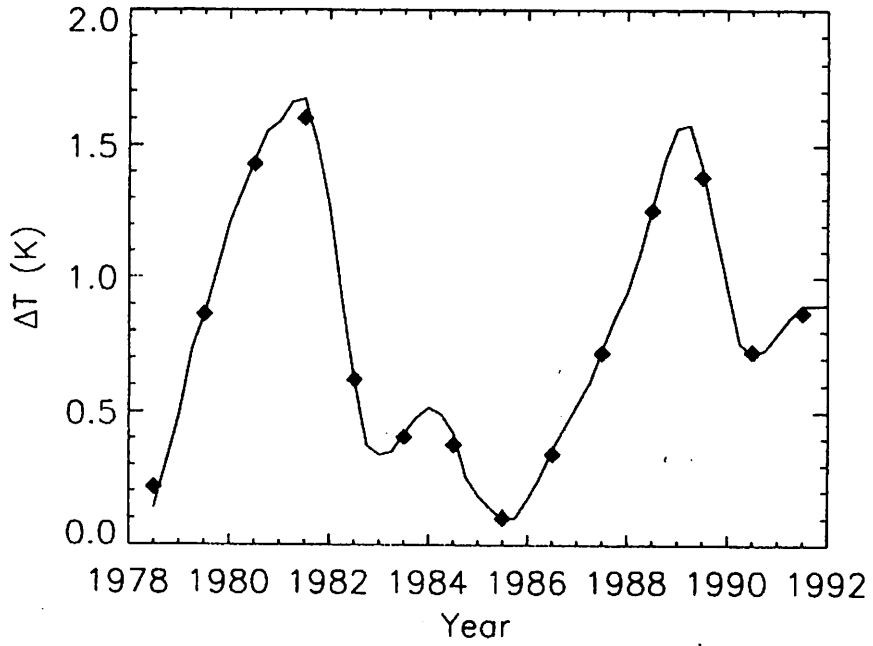
Figure 2. The measured solar photospheric temperature variations from 1978 to 1992 (Gray & Livingston, 1997) and the yearly mean.
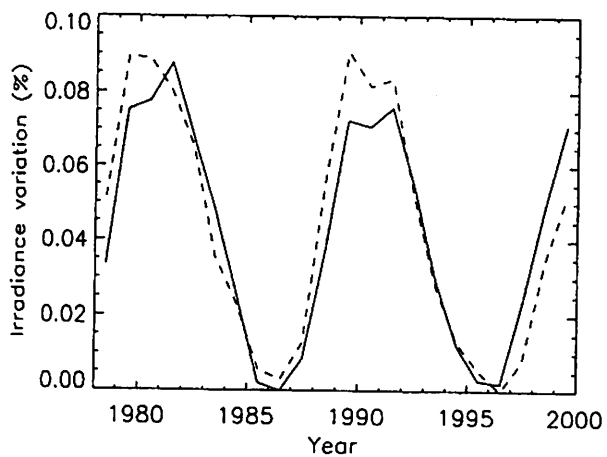
Figure 3. Comparison between the measured (solid curve) and calculated (dashed curves) solar irradiance variations.
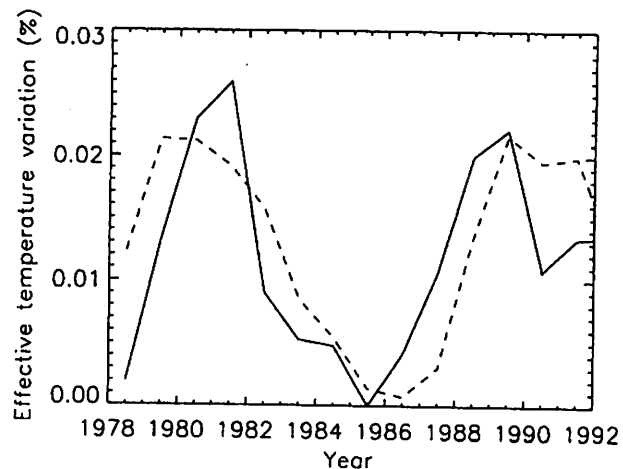
Figure 4. Comparison between the measured (solid curve) and calculated (dashed curve) solar photospheric temperature variations.
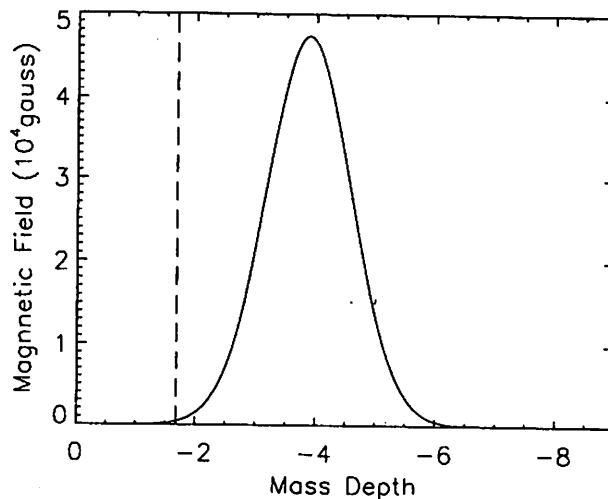
Figure 5. Distribution of the inferred magnetic field in the solar interior in 1989 according to the measured irradiance and photospheric temperature cyclic variations given in Figures 1 and 2. The vertical line indicates the base of the convection zone.

o. SOLAR TOTAL IRRADIANCE: 11 year cycle

b. SOLAR TOTAL IRRADIANCE: 11 year cycle + background
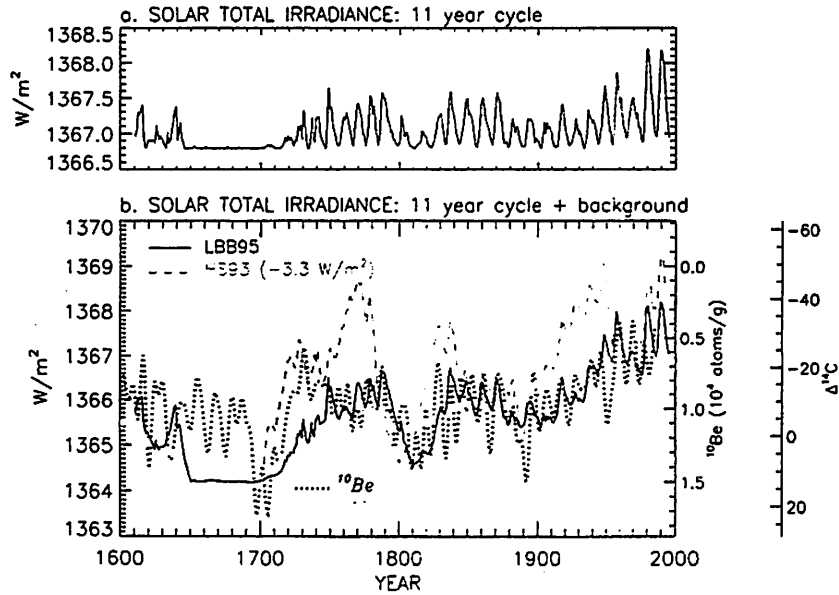
Figure 6 The reconstruction of solar total irradiance shown in (*a*) is of the 11-year cycle alone (Foukal & Lean 1990), whereas the dark solid line in (*b*) combines the 11-year activity cycle and a longer term component based on the average amplitude of each sunspot cycle (Lean et al 1995). This latter irradiance reconstruction is compared with ^{10}Be (*small squares*) and ^{14}C (*thick gray line*) cosmogenic isotope records (Beer et al 1988, Stuiver & Braziunas 1993) and with the Hoyt & Schatten (1993) irradiance reconstruction (*gray dashed line*) in which longer term changes are based on the length of the 11-year solar activity cycle (rather than average amplitude).
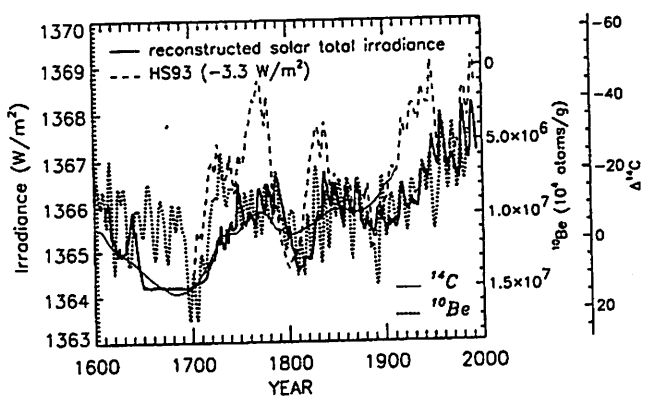
Figure 3. Tree-ring ^{14}C and ice-core ^{10}Be cosmogenic isotope records of solar variability are compared with reconstructed solar total irradiance and with the irradiance reconstruction of Hoyt and Schatten [1993] (HS93) which has a long term component based on Schwabe cycle length (rather than average amplitude).
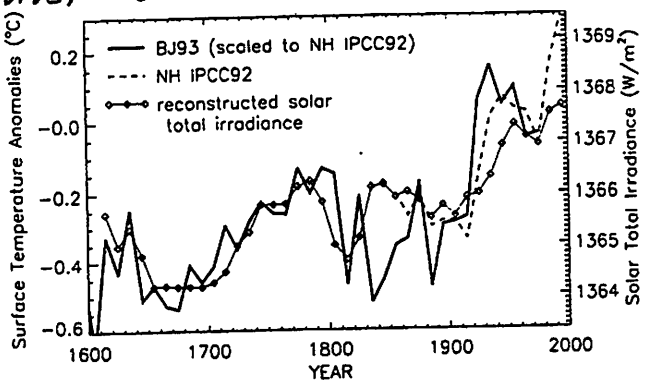
Figure 4. Compared are decadally averaged values of reconstructed solar total irradiance (diamonds) and NH temperature anomalies from 1610 to the present. The Bradley and Jones [1993] (BJ93) NH summer temperature anomalies (solid line) have been scaled to match the IPCC [1992] NH annual data (dashed line) during the overlap period.
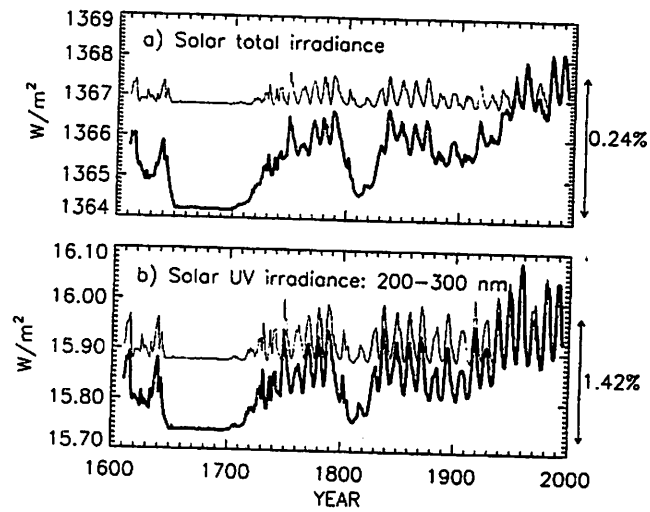
Figure 2. Reconstruction from 1610 to the present of (a) solar total irradiance and (b) UV irradiance in the band from 200 to 300 nm. In each panel the thin line is the irradiance variability of the Schwabe cycle, and the thick line is the Schwabe cycle plus a longer term variability component needed to account for the amplitude of irradiance reductions estimated independently for the Maunder Minimum (1645-1715) from observations of Sunlike stars.

Global-scale temperature patterns and climate forcing over the past six centuries

Michael E. Mann*, Raymond S. Bradley* & Malcolm K. Hughes†

* Department of Geosciences, University of Massachusetts, Amherst, Massachusetts 01003-5820, USA
† Laboratory of Tree Ring Research, University of Arizona, Tucson, Arizona 85721, USA

Spatially resolved global reconstructions of annual surface temperature patterns over the past six centuries are based on the multivariate calibration of widely distributed high-resolution proxy climate indicators. Time-dependent correlations of the reconstructions with time-series records representing changes in greenhouse-gas concentrations, solar irradiance, and volcanic aerosols suggest that each of these factors has contributed to the climate variability of the past 400 years, with greenhouse gases emerging as the dominant forcing during the twentieth century. Northern Hemisphere mean annual temperatures for three of the past eight years are warmer than any other year since (at least) AD **1400**.
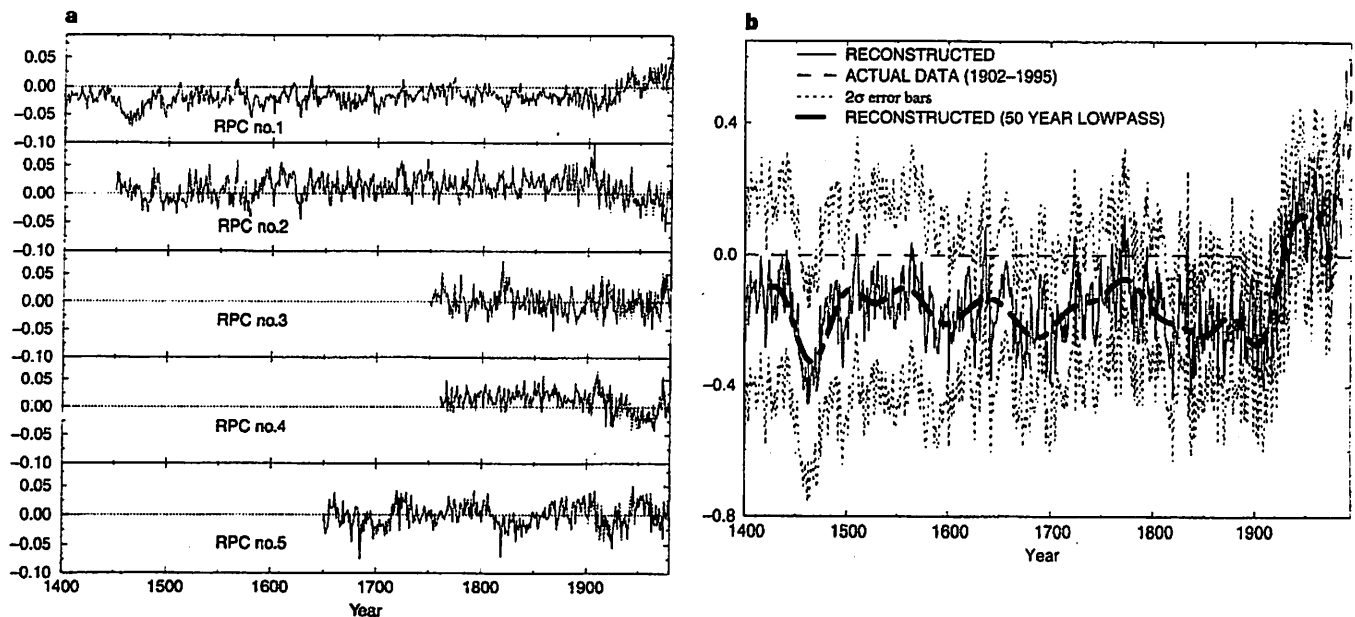
Figure 5 Time reconstructions (solid lines) along with raw data (dashed lines). **a**, For principal components (RPCs) 1-5; **b**, for Northern Hemisphere mean temperature (NH) in °C. In both cases, the zero line corresponds to the 1902-80 calibration mean of the quantity. For **b** raw data are shown up to 1995 and positive and negative 2σ uncertainty limits are shown by the light dotted lines surrounding the solid reconstruction, calculated as described in the Methods section.

V Long Term Studies

There is no solid reason to think that the variations of solar activity observed and inferred so far are the only variations of which the Sun is capable.

A direct study of solar activity for the next thousand years is needed:

To look for long term variations

To look for new tricks

In the meantime, monitor several hundred solar-type stars for the next hundred years.

O. C. Wilson, stellar activity cycles.

Sallie Baliunas, et al, Activity cycles and $\Delta S/S$ for 20 solar-type stars

HD 10476 shows decline of 0.6 percent in 5 years.

Tennessee State University monitors 160 solar-type stars.

NASA spacecraft to monitor more than 10^4 stars for 5 years.
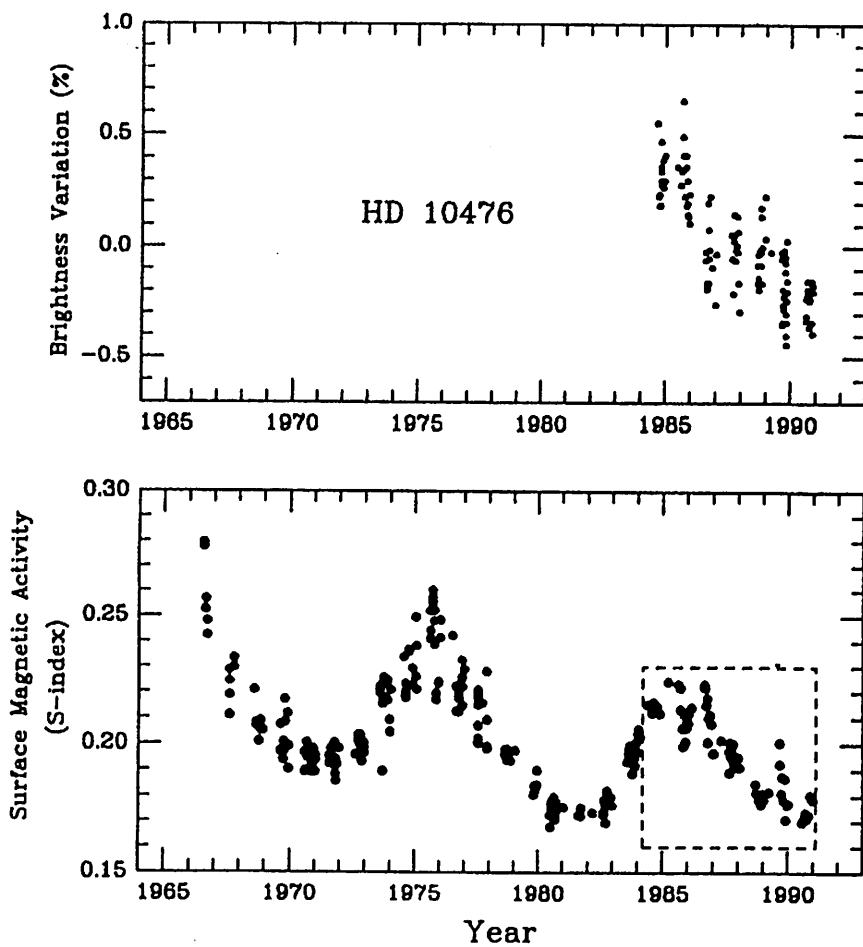
Fig. 1.—Records of the photometric brightness variation (nightly means) and surface magnetic activity (S index, the relative Ca II H and K emission flux, monthly means) for the star HD 10476. The dashed box in the bottom panel denotes the time interval of the concurrent photometric measurements shown in the upper panel.
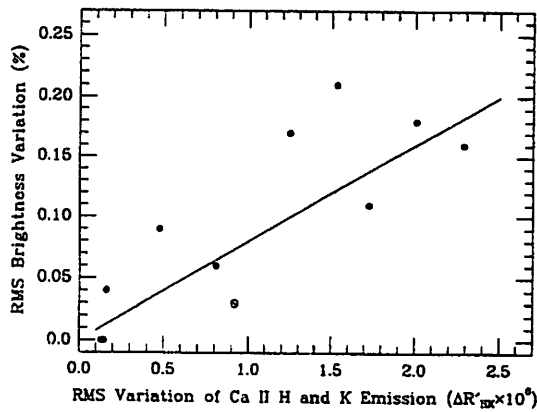
FIG. 2.—The rms variation in brightness (ΔBr in %) vs. the rms variation of excess chromospheric emission ($\Delta R'_{HK}$); the peak-to-peak variations are $\sim$3 times larger than the rms variations. For each star, the point connected to the origin represents the individual slope of the correlation between the activity and brightness variations. The solar data ($\odot$) are measurements of total irradiance from *SMM* satellite and Ca II K-line taken during 1980–1988 (Willson & Hudson 1991). The solid line represents the slope of the least-squares fit (eq. [2]).
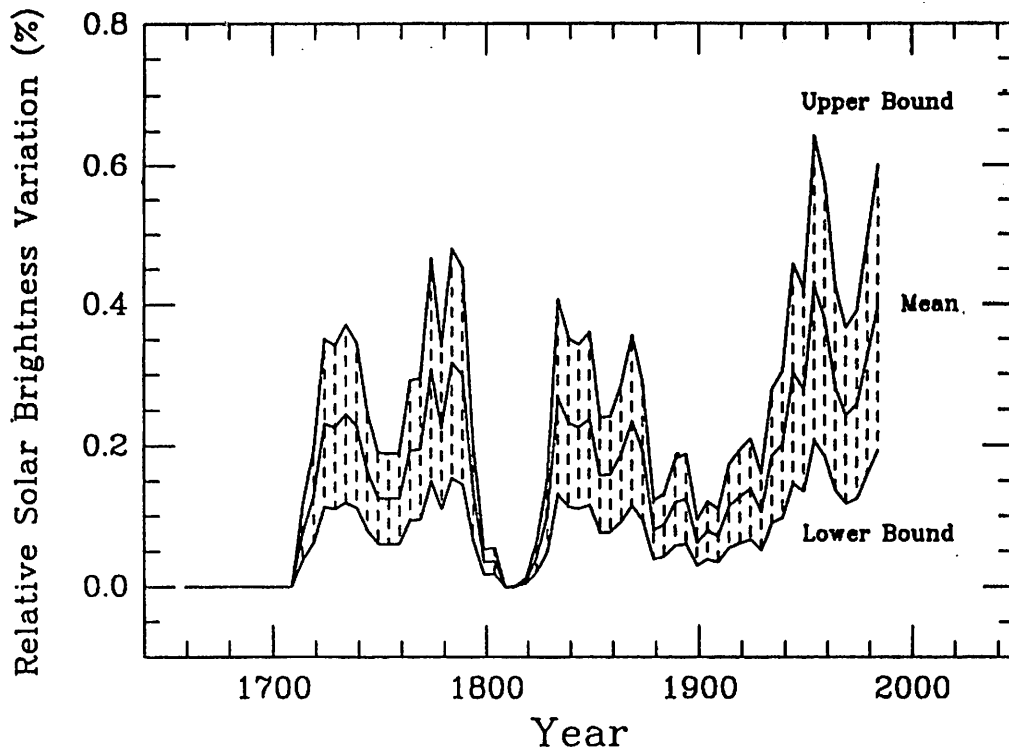
FIG. 3.—The relative change in solar brightness reconstructed using the 11 yr running mean of sunspot numbers and the brightness variation vs. the variation of surface magnetic activity relation of Fig. 2. The range of retrodiction of the solar brightness variation was calculated using the 95% confidence interval in the slope of eq. (2).

Fig. 1. Northern Hemisphere temperature anomalies from 1861 to 1989 (right-hand scale). The symbols (*) represent average values of the temperature record corresponding to individual solar cycles from solar maximum to solar maximum and from solar minimum to solar minimum, respectively. The second curve (+) shows the corresponding 11-year running mean values of the Zürich sunspot number (left-hand scale). For both curves, the abscissas of the plotted points correspond to the central time of the individual solar cycles.
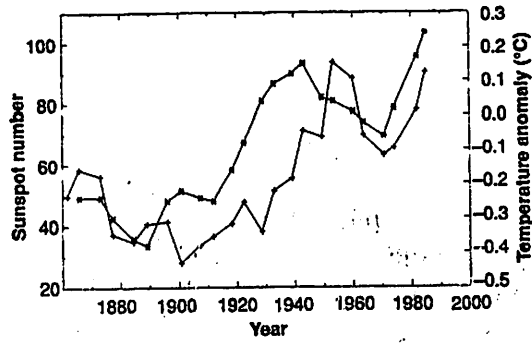
Fig. 2. Variation of the sunspot cycle length (left-hand scale) determined as the difference between the actual smoothed sunspot extremum and the previous one. The cycle length is plotted at the central time of the actual cycle (+). The unsmoothed last values of the time series have been indicated with a different symbol (*) which represents, as in Fig. 1, the Northern Hemisphere temperature anomalies.
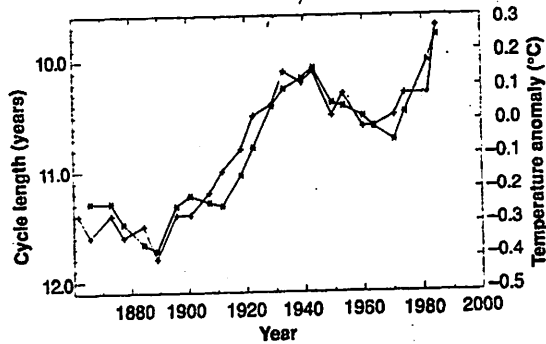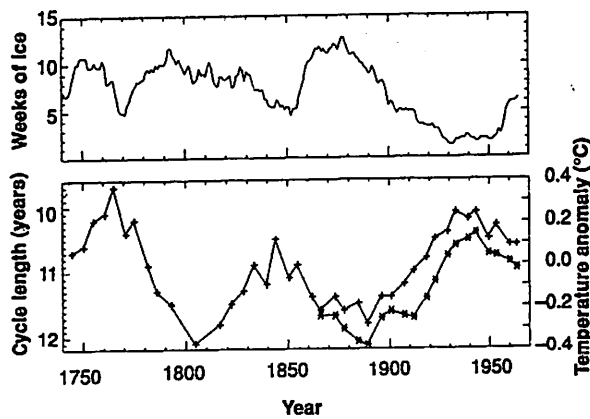
Fig. 3. (Top) 22-year running mean of the amount of sea ice around Iceland from 1740 to 1970 during summer months (represented by the number of weeks when ice was observed). (Bottom) Smoothed sunspot cycle lengths from 1740 to 1970 (left-hand scale) and Northern Hemisphere mean temperature (right-hand scale).

Terrestrial Records

    Ice cores

    Ocean bottom cores

    Terrestrial climate variations

Central role of a comprehensive global climate model.

    Solar variations and their influence on the ionosphere, stratosphere, troposphere.

    The coupling between the stratosphere and the troposphere

VI Theoretical Foundations?

Convection is hydrodynamics and provides the nonuniform rotation. Problem

Magnetohydrodynamics of the convection and nonuniform rotation provides the magnetic field. Problem

Effective diffusion of magnetic field. $10^{11} cm^2/cm$.

Partial list of mysterious phenomena:

1. Fibril state of the magnetic field

2. $0.5-1.0 \times 10^5$ Gauss at base of the CZ

3. Clustering of fibrils to form a sunspot

4. Sandwich structure of sunspot penumbra.

5. Internal structure of impulsive flare

6. The precise nature and origin of CME's

7. The vagaries of coronal heating

8. The precise origins of solar brightening

Solar activity is still in the exploratory stage.

VII Theoretical Problems

Hydrodynamics, nonuniform rotation

Magnetohydrodynamics of turbulent diffusion of magnetic field.

   Perhaps the individual magnetic fibril is the basic magnetic entity

   Buoyant rise of Ω-loops and 10^5 Gauss magnetic fields.

Theory needs all the observational guidance it can get.

This leads back to Solar B, and to the AST to investigate:

   Structure of the individual fibril

   Motions of individual fibrils

   Collective motions of fibrils

   Interactions of neighboring fibrils.
      very small flares

   Behavior of fibrils in association with prominences, surges, coronal mass ejections, flares, sunspots

   Time development of sunspot

   Internal structure of prominence

Internal structure of large flare.

Active heating in X-ray corona, and nanoflares.

This is the basis for X-ray astronomy of ordinary stars.